

TM-979  
1620-000



Fermilab

July 1980

SUPERCONDUCTOR MAGNETIZATION EFFECTS  
IN CORRECTION MAGNETS

D. Ciazynski

After the results obtained by R. Yarema during electrical measurements on correction magnets we decided to investigate the effects of the magnetization of the superconducting wire on the magnetic field provided by these magnets.

We were mainly interested in the case of the steering dipole inside the main quadrupole because the non-linearity was quite large and we had more data on this relatively simple case (two magnets without iron yoke).

1 - Electrical measurements

The measurements were made on a steering dipole (TSD-2) inside a main quadrupole (TQ-25) during tests of the power supply for the correction magnets. There was no current in the quadrupole.

a) Principle

For each test it was measured the voltage across the magnet (TSD):  $v_{\text{mag}}$ , the current in the magnet:  $i_L$  and the non-linear part of  $v_{\text{mag}}$  obtained by the following operation:  $\Delta v = v_{\text{mag}} - L \frac{di_L}{dt}$ .

$L \frac{di_L}{dt}$  was obtained from a separate circuit independent of the magnet.  $L$  could be adjusted close to the linear inductance of the magnet ( $L_m$ ). If we write:  $v_{mag} = L_m \frac{di_L}{dt} + v_{nl}$

So we have:  $\Delta v = (L_m - L) \frac{di_L}{dt} + v_{nl}$

The curves are shown figure 1, the current follows a triangular wave between  $+I_M$  and  $-I_M$ .

### b) Results

We can notice three important facts on these curves:

- 1) The non-linearity is quite large for  $I_m > 20A$
- 2) There is a sparkle at each  $dI/dt$  change
- 3) An odd phenomena happens for  $I=0$

### c) Discussion

It is interesting to make the numerical integration of the curves  $\Delta v(t)$  which gives in fact  $\Delta\phi(i_L)$ :

$$\Delta\phi(i_L) = (L_m - L) i_L + \Delta\phi_{nl}(i_L).$$

The curves (see fig. 2) are not very accurate and unfortunately the  $(L_m - L) i_L$  term cannot be cancelled even if we can draw  $\Delta\phi'(i_L) = \Delta\phi(i_L) + k i_L$  we cannot be sure to find exactly  $k = L - L_m$ .

However for  $i_L = 0$  we have  $\Delta\phi'(0) = \Delta\phi(0) = \Delta\phi_{nl}(0)$

remark:  $\Delta\phi$  is a flux across all the coils of the dipole and so we cannot calculate the magnetic field if we do not know the structure of this field.

We give below some values of  $\Delta\phi_{nl}(o)$

$I_m$ (A)	$dI/dt$ (A/s)	$(mWb) < \Delta\phi_{nl}(o) < (mWb)$	
5	20	12.2	13.3
10	40	24.7	27.6
22	45	72.6	79.8
45	36	109	145

To have a relative idea of these values we can give a rough value of the linear flux  $\phi_M = L_m I_M$  with  $L_m \approx 270$  mH.

$I_M$ (A)	$\phi_M$ (Wb)
5	1.35
10	2.70
22	5.94
45	12.20

Which gives:  $\frac{\Delta\phi_{nl}(o)}{\phi_M} \approx 1\%$

#### d) Conclusion

The shape of the  $\Delta\phi(iL)$  curves, the fact that  $\Delta\phi(o)$  does not seem to depend on the ramp rate show that this phenomena is certainly due to the magnetization of superconducting wire. This point will be studied in the following paragraphs.

## 2 - Basic Theory

We used the simple theory developed by M. A. Green <sup>1,2</sup> to determine the residual magnetic field due to persistent currents inside each filament. For more information one must see reference 1 and 2.

Using complex form<sup>3</sup> we can represent the residual field by:  $H' (Z) = H'y + i H' x$

with  $Z = x + iy$  (see Fig. 3)

The total field is  $H_t (Z) = H (Z) + H' (Z)$  where  $H (Z)$  is the field due to the transport current  $i_L$ .

For  $|Z| < R$ ,  $H' (Z)$  can be expanded as follows

$$H' (Z) = \sum_n a'_n Z^{n-1}$$

$$\text{with } a'_n = \frac{-D\beta}{4\pi(s+1)} \iint_{\sigma} J_c \epsilon r^n e^{-i(n+1)\theta} e^{i\alpha} dr d\theta \quad (1)$$

where:  $\sigma$  is the coil region

$D$ : the filament diameter (m)

$S$ : the metal to superconductor ratio

$\beta$ : the coil packing factor

$J_c = J_c (H_t)$  current density in superconductor (A/m<sup>2</sup>)

can also be written  $J_c (r, \theta)$ .

$\epsilon = \epsilon (H_t)$  doublet strength, can also be written

$\epsilon(r, \theta)$ . For fully penetrated filaments  $|\epsilon| = |\epsilon_0| = \frac{4}{3\pi}$

$$\alpha = \alpha (r, \theta) \text{ doublet angle: } = \frac{\pi}{2} + \theta + \tan^{-1} \left[ \frac{Bt\theta (r, \theta)}{Bt_r (r, \theta)} \right]$$

For  $\sigma$  defined by  $\theta_1 \leq \theta \leq \theta_2$   
 $R_1 \leq r \leq R_2$

we have: 
$$a'_n = \frac{-D\beta n}{4\pi(s+1)} \int_{R_1}^{R_2} r^{-n} dr \int_{\theta_1}^{\theta_2} \epsilon J_C \cos \left[ \frac{\pi}{2} - n\theta + \tan^{-1} \left( \frac{Bt\theta}{Bt_r} \right) \right] d\theta$$

( $a'_n$  : normal component)

or 
$$a'_n = \frac{-D\beta n}{4\pi(s+1)} \int_{R_1}^{R_2} r^{-n} dr \int_{\theta_1}^{\theta_2} \epsilon J_C \sin \left[ n\theta - \tan^{-1} \left( \frac{Bt\theta}{Bt_r} \right) \right] d\theta \quad (2)$$

This integration can be made numerically on all the coil regions:

$$a'_n = \frac{-D\beta n}{4\pi(s+1)} \Delta r \Delta \theta \sum_r r^{-n} \left( \sum_{\theta} \epsilon J_C \sin \left[ n\theta - \tan^{-1} \left( \frac{Bt\theta}{Bt_r} \right) \right] \right) \quad (3)$$

$B^i(Z) = \mu_0 H^i(Z)$  ( $\mu_0 = 4\pi \times 10^{-7}$ ) gives the harmonical analysis of the magnetic induction:  $B'_n = \mu_0 a'_n \times n^{-1}$

The  $\epsilon(H_t)$  function depends on the field penetration theory<sup>1-4,5</sup>, the  $J_C(Ht)$  curve is not well determined at low field<sup>6</sup> (< 1kG) and we must use fitting curves to approximate  $J_C(Ht)$  at low field.

### 3- Remanent field

For fully penetrated filaments ( $\Delta Ht > H_p$ ) we have  $\epsilon(Ht) = \epsilon_0 = \frac{-4}{3\pi}$

(second penetration). If we consider  $B' \ll B$  we can write from equation (3).

$$a'_n = \frac{-D\beta n \epsilon_0 \Delta r \Delta \theta}{4\pi(s+1)} \sum_r r^{-n} \left( \sum_{\theta} J_C(H) \sin \left[ n\theta - \tan^{-1} \left( \frac{B\theta}{Br} \right) \right] \right) \quad (4)$$

with  $\frac{B\theta}{Br} \neq f(I)$  but function of  $r$  and  $\theta$ .

If we suppose  $B = \sqrt{B_\theta^2 + B_r^2} \neq f(r, \theta)$  (that means the variation is not too large inside the coil and so we take an average value) we have  $J_c(H) = J_c(I) \neq F(r, \theta)$

If we apply equation (4) for  $I=0$  we obtain:

$$a'_n = \frac{-D\beta n J_{c0} \epsilon_0 \Delta r \Delta \theta}{\pi (s+1)} \sum_r r^{-n} \left( \sum_\theta \sin \left[ n\theta - \tan^{-1} \left( \frac{B\theta}{Br} \right) \right] \right) \quad (5)$$

with  $J_{c0} = J_c(0) = 10^{10} \text{ A/m}^2$

Theoretically this is not true because  $B(I) = 0$  for  $I=0$  and so  $B' \ll B$  is not fulfilled for  $I=0$ .

However we can have  $I \approx 0$  and still  $B' \ll B(I)$  and equation (5) is only an interpolation for  $I=0$ , more  $J_{c0}$  contains already the fact that  $Br(0) \neq 0$  but for the short sample.

#### a) E D/s dipole

Before using equation (5) to calculate the remanent field in the correction magnets we used it on the Energy Saver dipole. Only the main dipole field is counted in B here.

#### remanent field without iron yoke:

dipole component:  $B_1 = 5.0 \text{ G}$

sextupole field at  $x=1''$ :  $B_3(1'') = 5.6 \text{ G}$

or  $B_3(1'')/B_1 = 1.12$

#### remanent field with iron yoke (according to ref. 2)

dipole component:  $B_1 = 4.0 \text{ G}$

sextupole field at  $x = 1''$ :  $B_3(1'')/B_1 = 1.21$

Before doing comparisons with the measurements one must think that we used a two dimensional model and we counted only the residual current inside each filament. The measured values given below come from reference 7 and 8.

magnets with iron yoke:

$$\begin{aligned} \text{E 5 - 1}^7 \text{ (5' long): } \quad B_1 &= 12 - 2.5 = 9.5 \text{ G} \\ B_3 &= 10.7 \text{ G at } x= 1'' \\ \text{or } B_3(1'')/B_1 &= 1.13 \end{aligned}$$

$$\begin{aligned} \text{E 22 - 1A}^8 \text{ (22' long): } \quad B_1 &= 8.5 - 2.5 = 6.0 \text{ G} \\ B_3 &= 7.15 \text{ G at } x= 1'' \\ \text{or } B_3 (1'')/B_1 &= 1.19 \end{aligned}$$

magnet without iron yoke:

$$\text{E 5 - 2 (5' long): } \quad B_3 = 10.3 \text{ G at } x= 1''$$

remark 1: As shown in ref. 7 (fig. 12) and ref. 8 (fig. 14) the remanent field increases at the ends.

remark 2: As shown in ref. 7 (fig. 14) one must decrease the values of about 7% to obtain the field due to currents inside filaments only and the results also depend on how the power supply is shut off.

The calculated values are not bad but always lower than the measurements.

b) steering dipole inside a main quadrupole

The magnets are mounted without iron yoke. We suppose that we have fully penetrated filaments.

steering dipole (alone): We used all the harmonics ( $n \leq 20$ ) to calculate B and so  $\alpha(r, \theta)$ .

$$\text{dipole remanent field: } \underline{\underline{B_1 = .30 \text{ G}}}$$

Harmonic analysis of the remanent field at  $x= 1''$

$n = 2k+1$	$B_n/B_1$
1	1.0
3	1.68
5	-1.20-01
7	-8.02-02
9	1.27-01
11	-2.07-02

The dipole component is low ( $< 1 \text{ G}$ ) but the sextupole component is relatively high.

main quadrupole: Without current and in the field of the dipole.

dipole remanent field:  $B_1 = \underline{13.4 \text{ G}}$

Harmonical analysis at  $x= 1''$

$n = 2k+1$	$B_n/B_1$
1	1.0
3	0
5	1.22-01
7	0
9	-7.84-03

remark 1: Although the magnet has a "quadrupole symmetry" the exciting field is a dipole field which will give dipole remanent field because the connections of the wires do not count in this effect.

The dipole remanent field is high ( $> 10 \text{ G}$ ), the sextupole is canceled by the coil geometry.

The results for the total remanent field are given below

$n = 2k+1$	$B_n$ at $x= 1''$ (G)	$B_n/B_1$ at $x=1''$
1	13.7	1.0
3	5.04-01	3.68-02
5	1.59	1.15-01
7	-2.41-02	-1.76-03
9	-6.70-02	-4.89-03

The remanent field due to TSD is negligible to compare with the field due to the quadrupole.

remark 2: If  $I_{TQ} = c^{te} \neq 0$  the results will be affected as follows ( $\Delta B$  value for  $I_{TQ}=0$ ,  $\Delta B'$  value for  $I_{TQ} \neq 0$ ).

$$I_{TQ} \neq 0 \Rightarrow J_{TQ} = \frac{4 (s+1) I_{TQ}}{23 \pi d^2} \neq 0$$

(d: strand diameter)

if  $\delta = \frac{J_{TQ}}{J_c(B_Q)}$       B: magnetic field due to  $I_{TQ} = B(r, \theta)$   
 $B_D$ : average value of B on TSD  
 $B_Q$ : average value of B on TQ

TSD field:  $\Delta B' = \Delta B \frac{J_c(B_D)}{J_c(O)}$

TQ field:  $\Delta B' = (1-\delta) \Delta B \frac{J_c(B_Q)}{J_c(O)}$

$I_{TQ}$ (A)	$(\Delta B'/\Delta B)$ (TSD)	$(\Delta B'/\Delta B)$ (TQ)	$(\Delta B'/\Delta B)$ tot
2500	.42	.31	.31
4250	.34	.16	.17

For  $I_{TQ} = 4250$  the remanent field becomes more reasonable (2.3G).

Comparison with electrical measurements.

To make some comparisons we need to know the magnetic flux across the dipole coils. If we neglect the field due to the steering dipole this calculation is easy.

If  $B'n$  is the residual field at 1" and  $\Delta\phi_n$  the corresponding flux (harmonic  $n$ ) we obtain:

$$n = 2k+1: \Delta\phi_n = \frac{4L}{Sn^2} \frac{1}{n+2} (R_2^{n+2} - R_1^{n+2}) \sin n \theta_0 \frac{\Delta Bn}{R_0^{n-1}}$$

with:  $\theta_0$ : dipole coil angle =  $\pi/3$

L: coil length  $\approx 65''$

S: strand cross section (dipole coil)

$R_1$  ( $R_2$ ): inner (outer) radius of TSD

$R_0 = 1''$  reference radius

so we have  $\Delta\phi_R(o) = \sum_n \Delta\phi_n$

n	$\Delta\phi_n$ (mWb)
1	83
3	0
5	-1.9
7	0
9	0

These values give  $\Delta\phi_R(o) = \underline{81 \text{ mWb}}$  which is lower than the value obtained from electrical measurements  $109\text{mWb} < \Delta\phi(o) < 145 \text{ mWb}$  but which is not so bad (see §3a for remarks).

#### 4 - Magnetization curves

Using a simple field penetration theory <sup>1,2</sup> we can obtain magnetization-like curves  $B' (I)$  where  $B'$  is the residual field.

Equation (5) will be still used for the quadrupole which provides the main part of the residual field.

$$a'_n = - \frac{D\beta n J_c \epsilon \Delta r \Delta \theta}{4\pi (s+1)} \sum_r r^{-n} \left( \sum_{\theta} \sin \left[ n\theta - \tan^{-1} \left( \frac{B\theta}{Br} \right) \right] \right)$$

$$\text{in fact we studied } \eta (I) = \frac{B' (I)}{B'_m (0)} = \frac{J_c(B)}{J_{c0}} \frac{\epsilon(B)}{\epsilon_0}$$

$B'_m (0)$  is  $B'_{\max} (0)$  obtained for fully penetrated filaments we have in fact  $\eta(I) = \eta (I, I_m)$ .

$$\text{We took } J_c(B) = \frac{J_{c0} B}{B + B_0} \quad \text{with } B_0 = 1T \\ J_{c0} = 10^{10} \text{ A/m}^2$$

$\epsilon(B)$  depends on the penetration history (see ref. 1): for the "linear penetration" model and for the first penetration we

$$\text{have } \epsilon = \epsilon_0 (2k - k^2)^{\frac{3}{2}} \\ \text{with } \epsilon_0 = \frac{4}{3\pi} ; k = \frac{2dp}{D} \quad \text{and } dp = \int_0^B \frac{dB}{\mu_0 J_c(B)} \quad (k \leq 1)$$

the penetration field ( $k=1$ ) is  $B_p \approx \frac{\mu_0 J_c (0) D}{2} \approx 0.5 \text{ kG}$

The calculated curves are shown figures 4 and 5.

- 1 - These curves give the general shape seen Fig. 2
- 2 - They do not explain what happens for  $I \approx 0$
- 3 - The shape of the curve at  $I_{\max}$  is not proper
- 4 - The penetration field is certainly closer to 1KG than 0.5 kG (which was found for the ED/S dipole too)?

We can improve the third point by using a radial penetration model which is closer to the real life<sup>9</sup>. This improvement can be seen figure 6 where we studied  $\Delta v$ .

$$\Delta v = \frac{d}{dt} (\Delta\phi) = A \left( \frac{dB'}{dI} \right) \cdot \left( \frac{dI}{dt} \right)$$

$$\text{with } A = \frac{4L}{3S} (R_2^3 - R_1^3) \sin \theta_0 = \frac{2L}{\sqrt{3} S} (R_2^3 - R_1^3) \quad (\text{see §3-b})$$

for a triangular wave  $\left( \frac{dI}{dt} \right) = -c^{te}$  when I comes from  $I_m$  to  $-I_m$

If one want to explain the real shape of the curves for  $I \approx 0$  one need to use a more complicated theory (  $J_c(H)$  must be drastically charged at low field, the concept of coherence length must be introduced )<sup>9</sup>.

We can have a good idea of what a more sophisticated theory can give by looking at ref. 5, figure 7 is extracted from this report. So we can conclude that the phenomena seen at  $I \approx 0$  is really due to the magnetization of the superconducting wire.

## 5 - Discussion

A relatively simple theory of the superconductor magnetization enabled us to explain some experimental results giving good values for the remanent field produced by this phenomena.

To explain the entire magnetization curve one need a more real model of the field penetration in the superconductor.

We can give a summary of the main results.

The main part (97%) of the dipole remanent field is in fact due to the qudrupole wire. This field is about 15 G for  $I_{TQ} = 0$  and should be reduced to 5 G for  $I_{TQ} = 2500$  A and to

3 G for  $I_{TQ} = 4250A$ .

- The shape of the  $\Delta v(t)$  curves can be explained by the theory and so the main part of the non-linearities is due to the superconducting wire.

- The remanent field due to the steering dipole alone is low (dipole field  $\sim 0.5G$ ) but the sextupole field is relatively high ( $B_3(1'')/B_1 = 1.68$ ).

## 6 - Conclusion

As the steering dipole will be put now outside the main quadrupole, the original problems treated in this report have no more interest. However, with this dipole put in a package with a quadrupole and a sextupole the same kinds of problems will happen for these three coils.

In this package the remanent field due the iron shield has to be considered too. The first magnetic measurements on the TCP magnets<sup>10</sup> showed relatively high values of the remanent fields but they need to be confirmed.

The main problems due to the magnetization of the superconducting wire are:

- The non-linearity of the main field  $B(I)$  at low current
- The sextupole residual field for the steering dipole at low field.

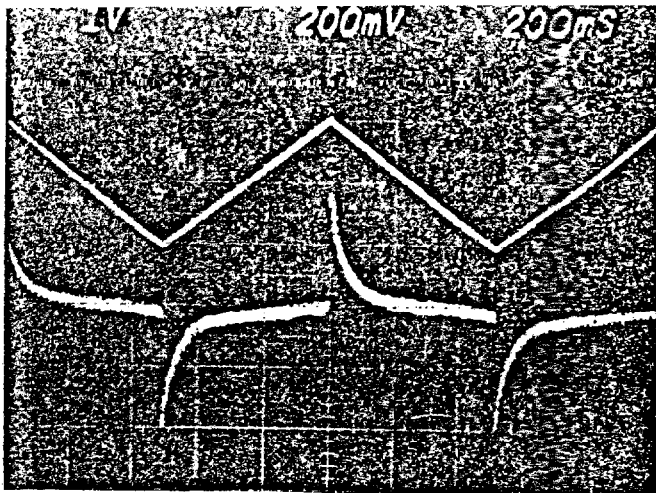
We will make calculations on the new design correction magnets but we will need accurate magnetic measurements at low field for these magnets.

References

1. M. A. Green: UCID3508 (1971) LBL
2. M. A. Green: Brookhaven Magnet Conference (1972)
3. R. A. Beth: Jnl of Applied Physics vol. 37 nr 7 (1966) p. 2568
4. H. Inhaber: Cryogenics, May 1973, p. 261-271
5. J. J. Wollan and M. C. Ohmer: Cryogenics, May 1976, p. 271-280
6. M. R. Daniel and M. Ashkin: Cryogenics, May 1976
7. R. Yamada, H. Ishimoto, M. Price, R. E. Peters: TM-667 (1976)
8. R. Yamada, H. Ishimoto, M. Price: TM-726 (1977)
9. M. A. Green: Private communication
10. D. Ciazynski: Test of TCP - 4 at Lab 5.

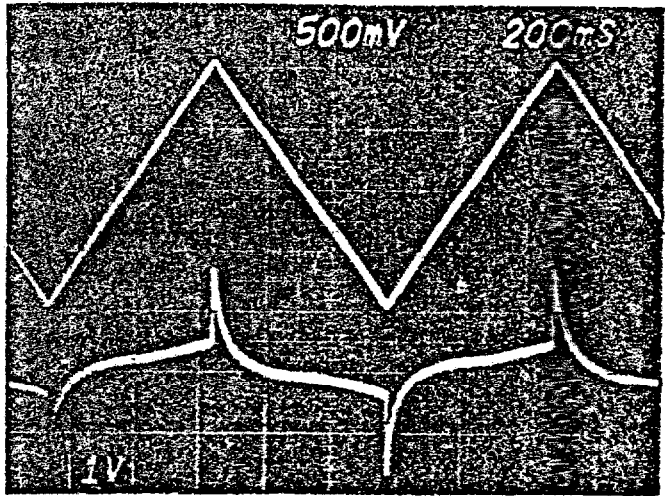
$I_L : 5A/div$

$v : .2V/div$



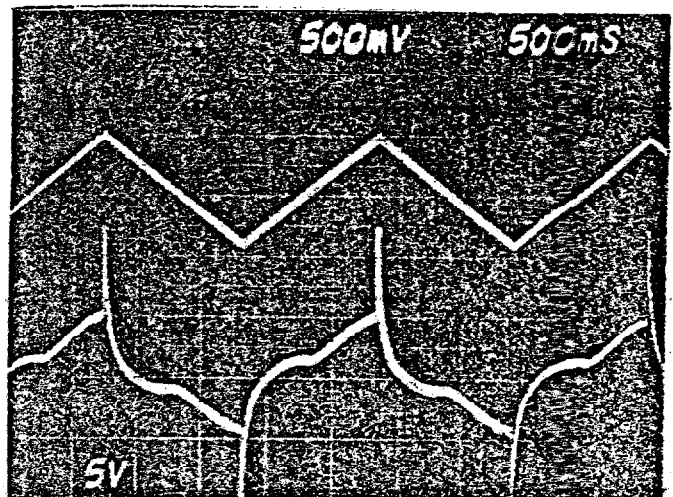
$I_L : 5A/div$

$v : .5V/div$



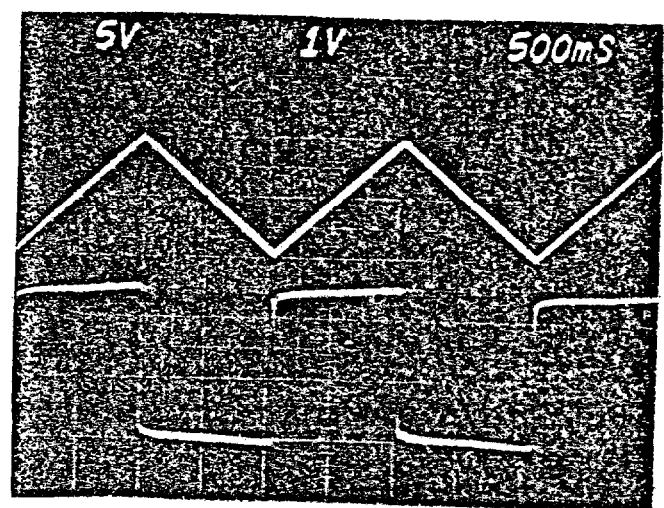
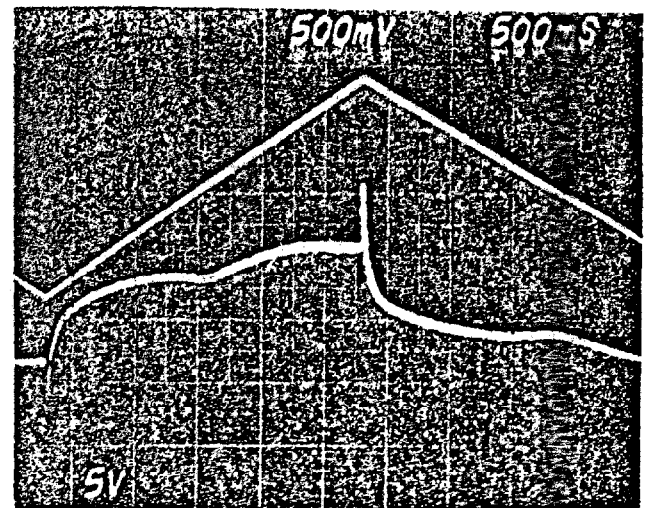
$I_L : 25A/div$

$v : .5V/div$



$I_L : 25A/div$

$v : .5V/div$



$v_{mag} : 10V/div$

Figure: 1

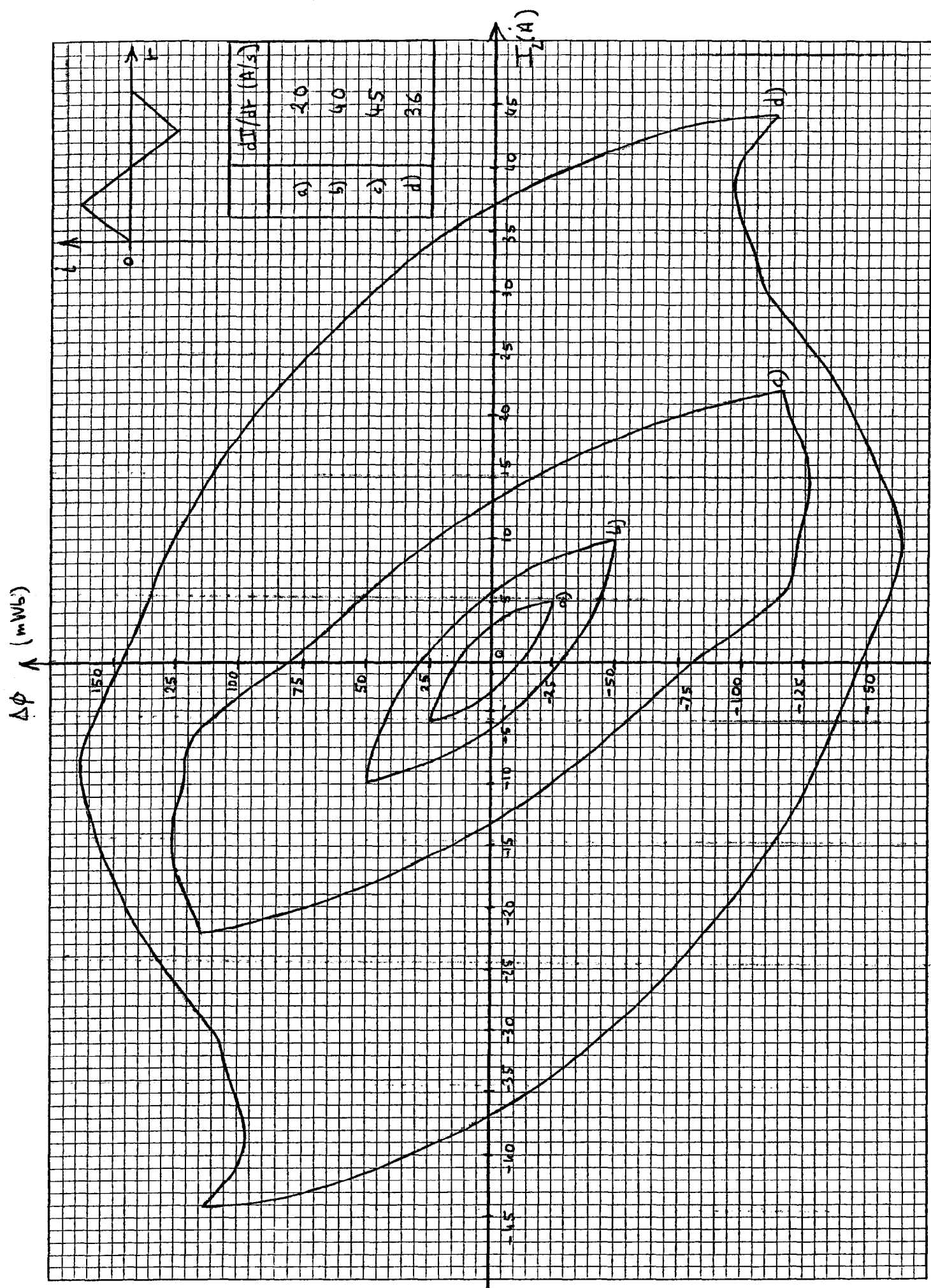


Figure:2

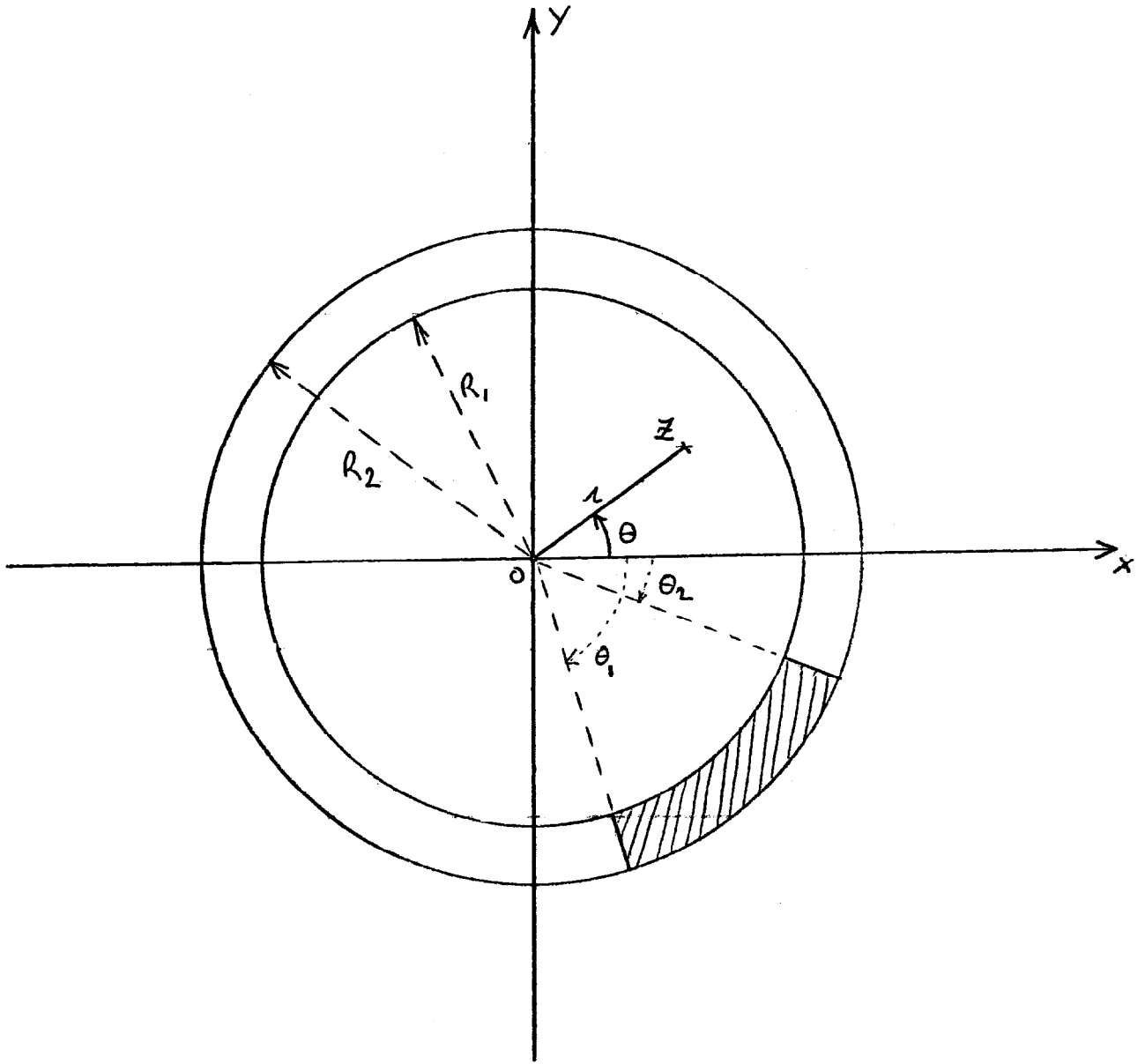


Figure:3

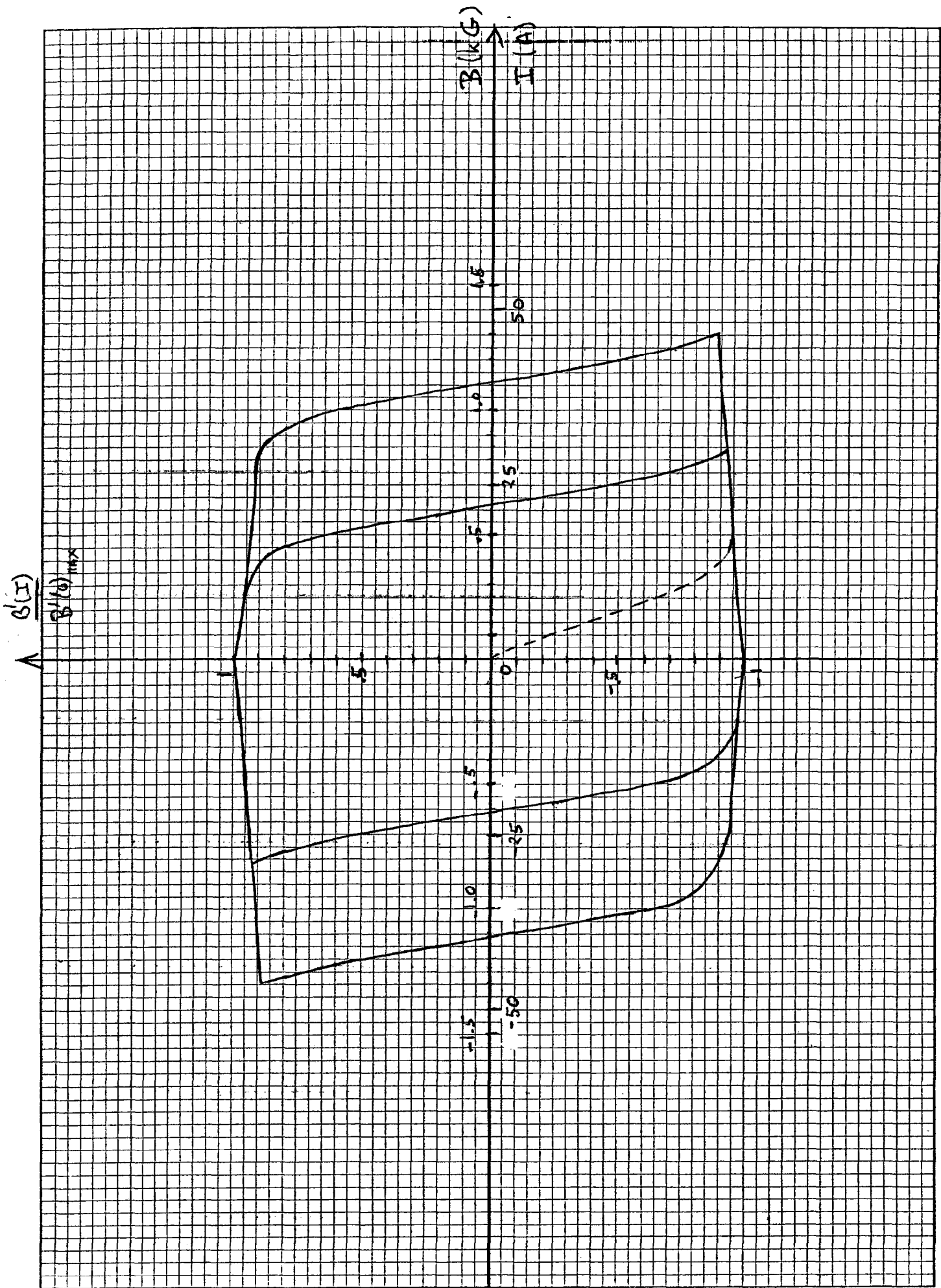


Figure:4

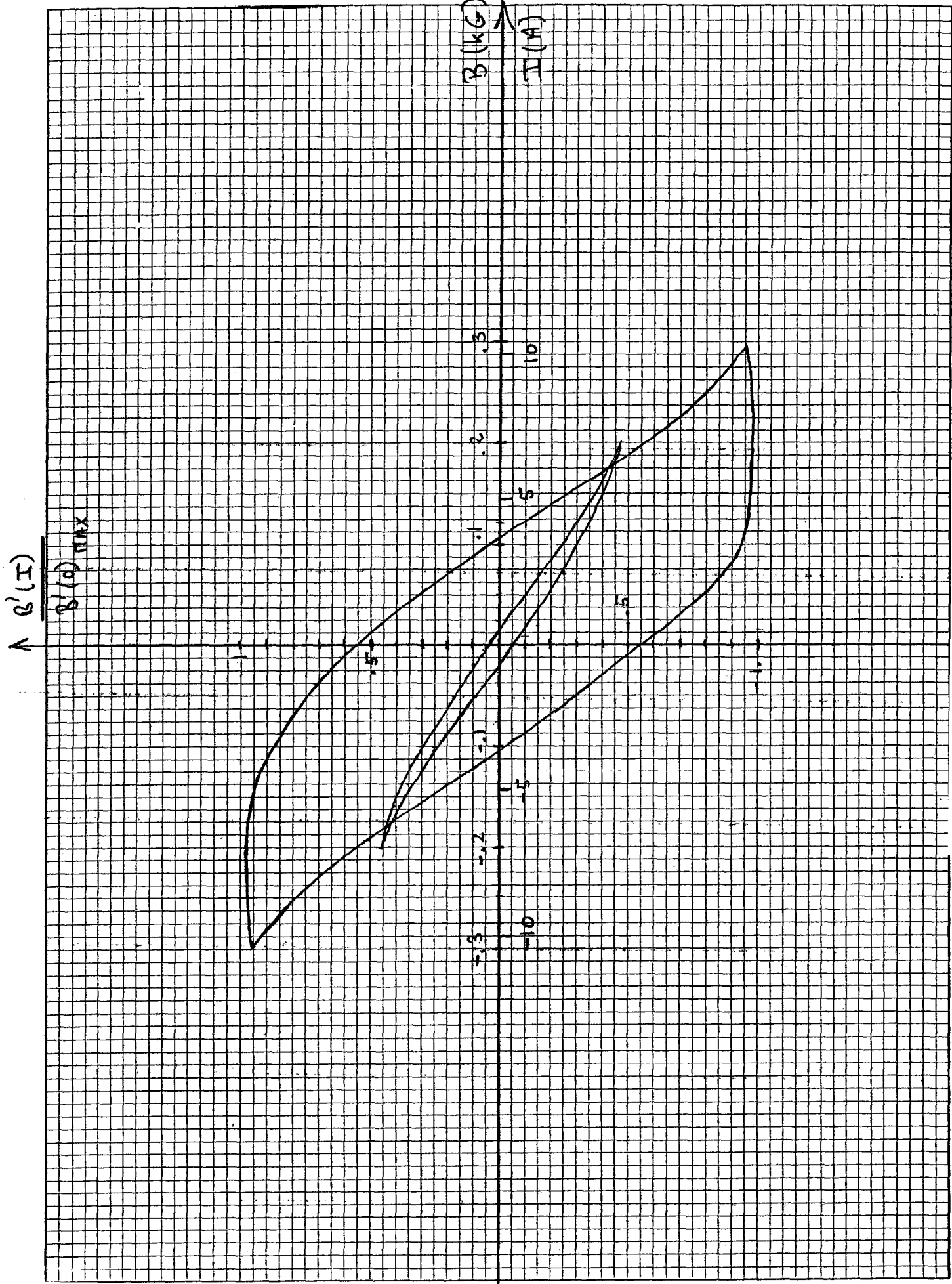
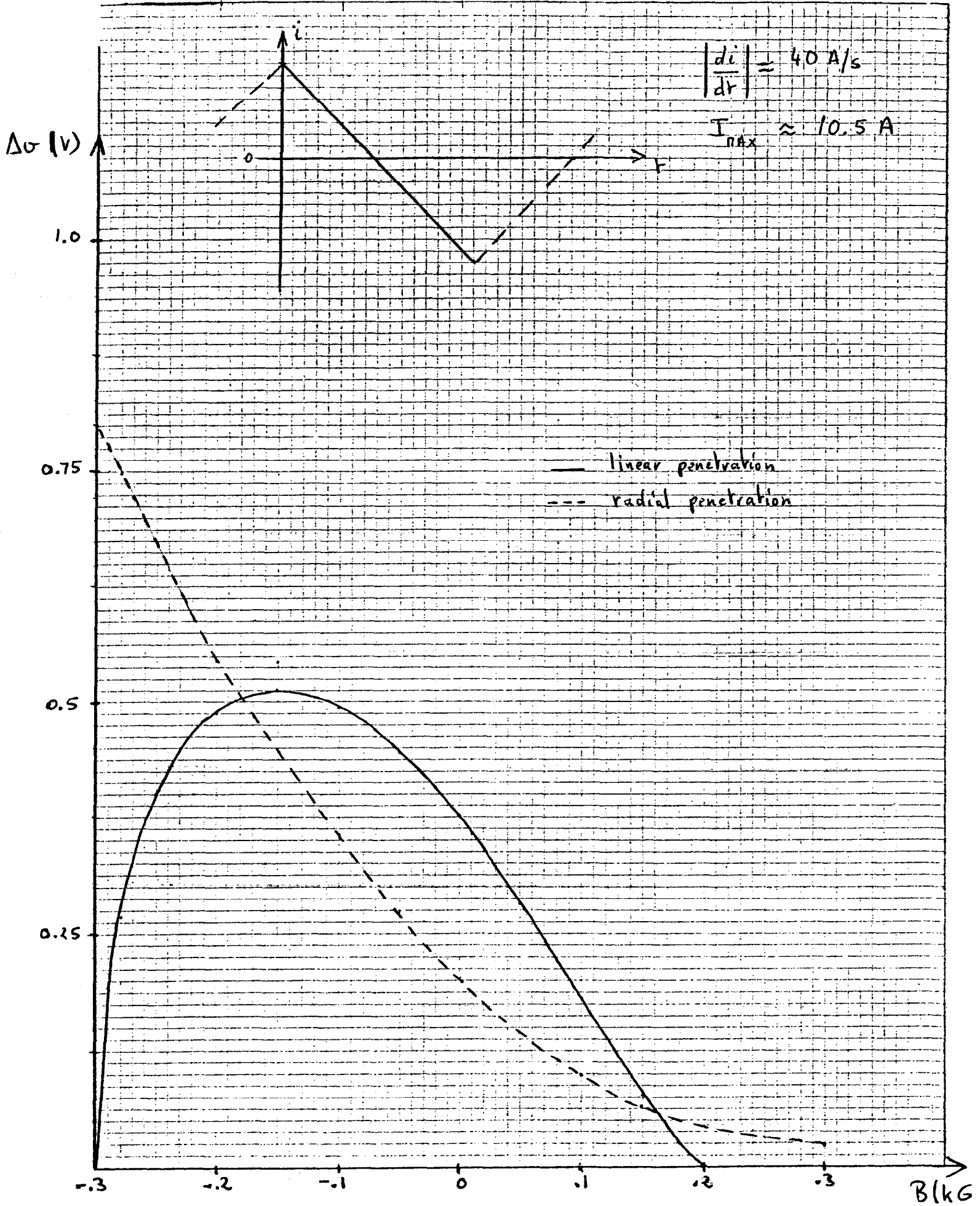


Figure : 5

Figure: 6



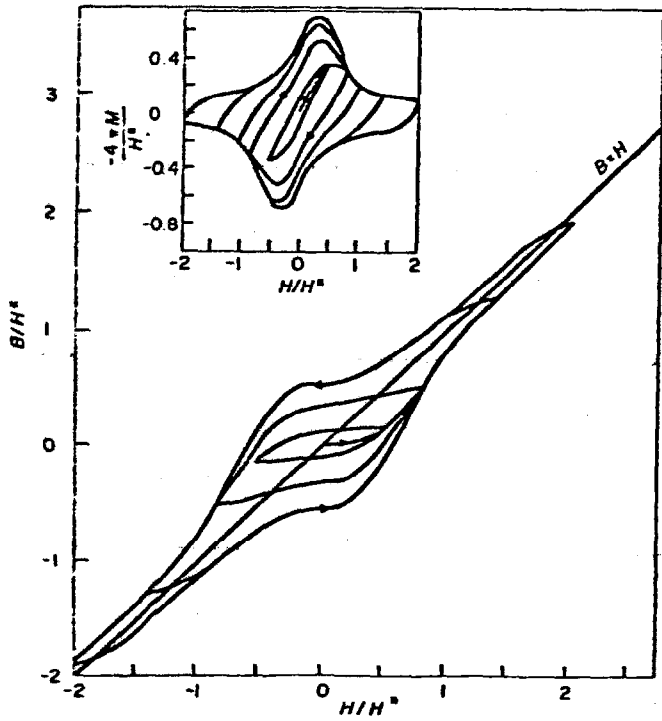


Fig. 2 Full-cycle hysteresis loops for  $h_m = 0.5, 0.8, 1.4,$  and  $2.0$ ; reduced magnetic induction versus reduced magnetic field and reduced magnetization versus reduced magnetic field (insert) for the alpha model

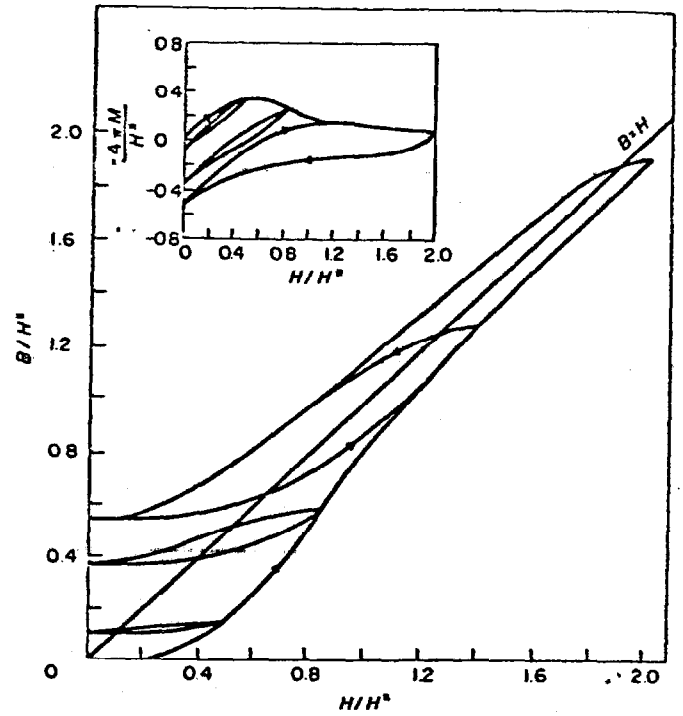


Fig. 3 Half-cycle hysteresis loops for  $h_m = 0.5, 0.8, 1.4$  and  $2.0$ ; reduced magnetic induction versus reduced magnetic field and reduced magnetization versus reduced magnetic field (insert) for the alpha model

Figure: 7 (From reference 5)